Optimizing 4D fluid imaging

A. T. McInally[1], T. Redondo-López[1], J. Garnham[2], J. Kunka[1], A. D. Brooks[1], L. Stenstrup Hansen[3], F. Barclay[4] and D. Davies[4]

[1]*Enterprise Oil Plc, St. Magnus House, Guild Street, Aberdeen AB11 6NJ, UK (present address: Shell Exploration and Production UK, 1 Altens Farm Road, Nigg, Aberdeen AB12 3FY, UK)*
[2]*Enterprise Oil Plc, St. Magnus House, Guild Street, Aberdeen AB11 6NJ, UK*
[3]*Ødegaard A/S, Titangade 15, DK-2200 Copenhagen N, Denmark*
[4]*Ødegaard U.K. Ltd, West Lodge, 12 Greenwell Road, Aberdeen AB12 3AX, UK*

ABSTRACT: Integrated analysis of 4D seismic data and petrophysical data is used to produce probabilistic fluid and lithology volumes for monitoring reservoir performance on the Nelson Field. Petrophysical analysis of log data shows distinct fields for oil sand, water sand, shale and heterolithic 'lithologies' in acoustic impedance – Poisson's ratio space. Elastic inversion techniques applied to conventional 4D AVO datasets convert the reflectivity data to acoustic impedance, shear impedance, Poisson's ratio and angle impedances. The elastic inversion datasets are used to quantify oil–water contact movements through volume sculpting techniques. Well-derived relationships are used to predict 3D volumes of oil sand probability from three different seismic survey vintages: 1990, 1997 and 2000. Changes in oil sand probability due to production are verified by comparison with repeat production logs. Integrated volume interpretation of 4D far offset inversion difference (oil–water contact (OWC) movement) and oil sand probability shows areas of unswept oil, highlighting infill opportunities. Early results from infill drilling have validated the method, realizing the potential economic benefits of 4D seismic technologies.

KEYWORDS: *4D, AVO, elastic inversion, reservoir characteristic*

INTRODUCTION

The application and technology of 4D or 'time-lapse' seismic data to field development has developed rapidly since the mid to late 1990s (Jack 1998; Koster *et al.* 2000; Parr *et al.* 2000; Boyd-Gorst *et al.* 2001). The Nelson Field is a perfect candidate for using 4D seismic technology for reservoir management, and was the site of one of the first dedicated marine 4D surveys, acquired in 1997 (Harris & Henry 1998), helping to prove the feasibility of the technique. The field lies in Blocks 22/11, 22/6a, 22/7 and 22/12a in the UK Central North Sea, 180 km east of Aberdeen in approximately 85 m (280 ft) of water. It is one of a series of Paleocene oil accumulations situated on the Forties–Montrose High in the Central North Sea (Fig. 1), a region of elevated Permian and Devonian basement (Ahmadi *et al.* 2003). Nelson is a simple four-way dip closed structure situated at a depth of approximately 2195 m (7200 ft) below mean sea-level. The Nelson reservoir occurs within the Forties Sandstone Member of the Sele Formation. The field was discovered in the mid 1980s (see Whyatt *et al.* 1992) and was brought on stream in 1994. To date, the field has produced 330×10^6 STB oil equivalent (BOE). Seismic data over the field are of excellent quality and were used as a tool for reservoir characterization and to track fluid movements caused by production. This was achieved through the acquisition of specific repeat 3D surveys and the application of elastic inversion. This paper demonstrates the work flow employed by

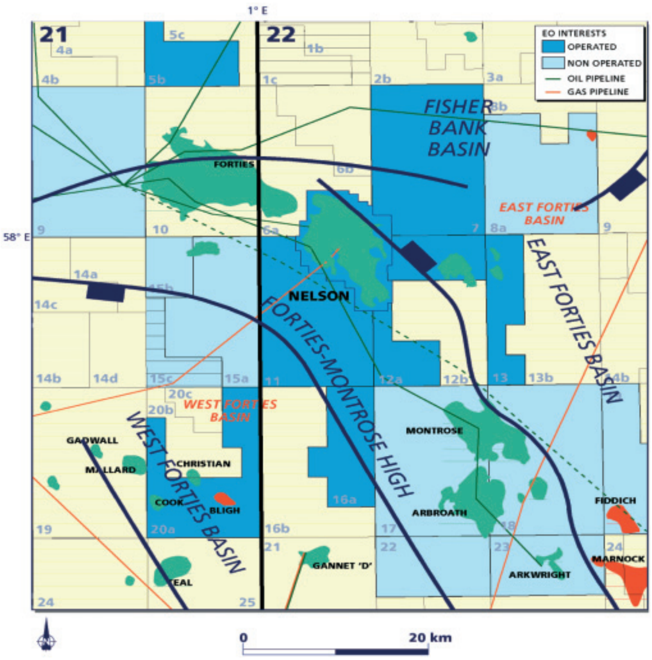

Fig. 1. The location of the Nelson Field, UK Central North Sea.

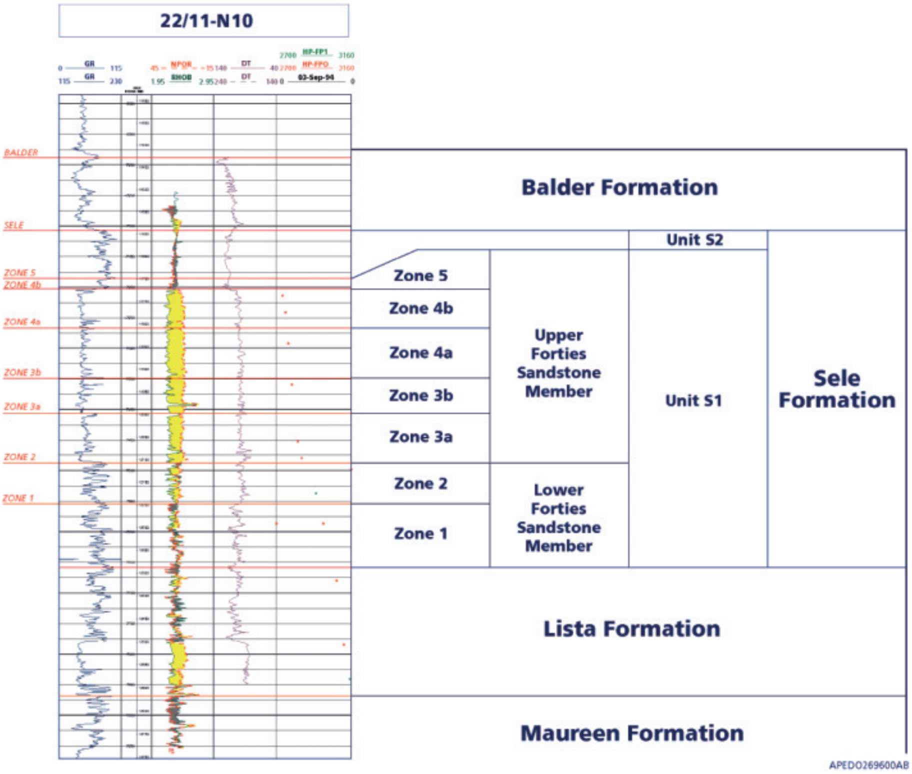

Fig. 2. Nelson Field stratigraphy and reservoir zonation.

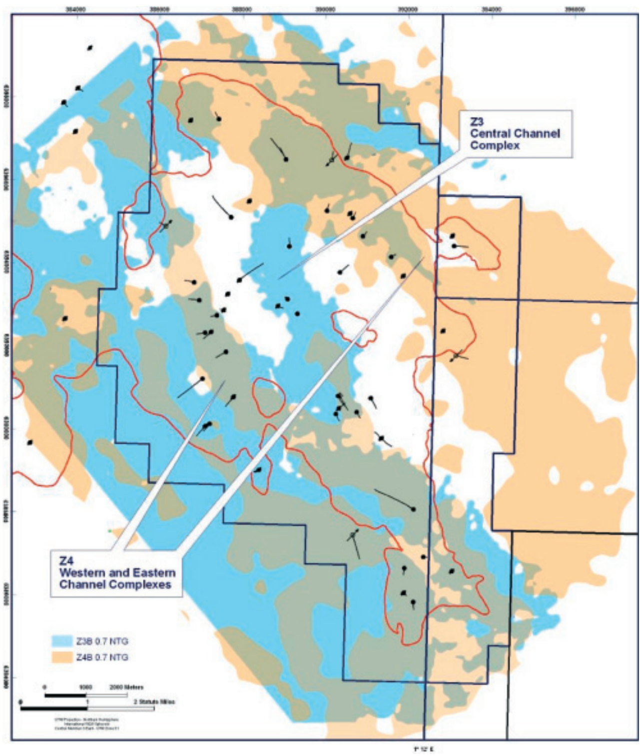

Fig. 3. The Western, Central and Eastern Channel complexes overlain on the Nelson Field outline.

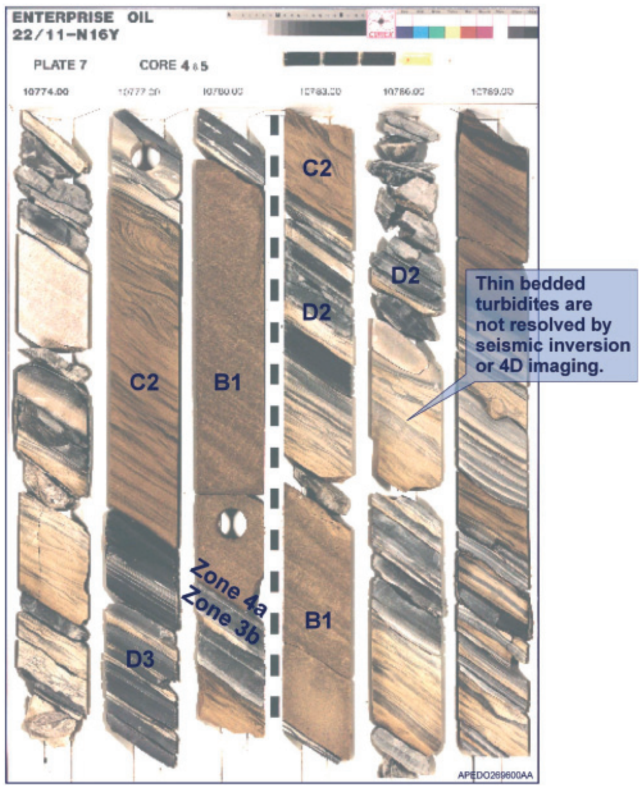

Fig. 4. Nelson Channel Margin core facies, from Nelson production well N16y. Facies comprise interbedded sandstones, siltstones and mudstones, deposited by high and low density turbidity currents.

the Nelson Reservoir Development Team to optimize fluid and lithology imaging using 4D seismic data. The main aim of the work was to aid the targeting of infill well opportunities on the field. Optimized fluid and lithology imaging was achieved through a combination of seismic modelling, detailed petrophysical analysis of well log and core data, and elastic inversion of 4D seismic data.

RESERVOIR GEOLOGY

The Paleocene Forties Sandstone Member, which occurs within Sele Unit S1 (Knox & Holloway 1992), was deposited in the confined Central Graben as a sand-rich, sheet-like, basin floor

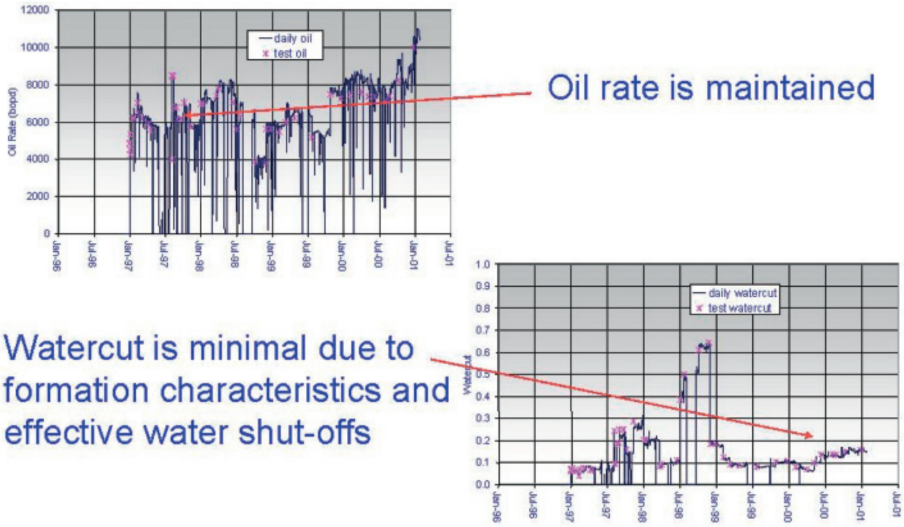

Fig. 5. The production characteristics of the channel margin facies association, well N16y.

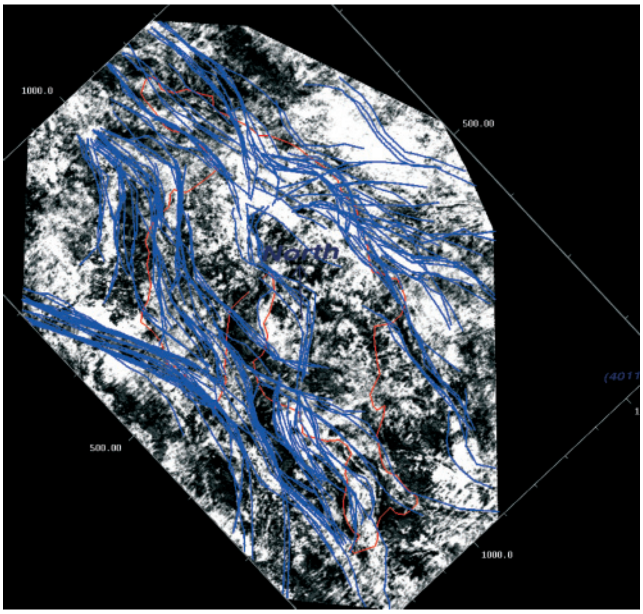

Fig. 6. Near-offset Attribute Convergence display illustrating the high impedance contrast of the Forties Sandstone Formation allowing sediment fairways to be mapped readily.

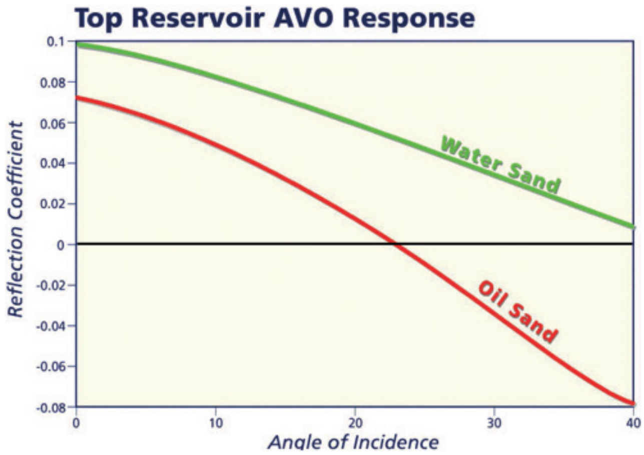

Fig. 7. Top Forties Formation AVO response to oil and water fills (from Boyd-Gorst *et al.* 2001).

sand system (Den Hartog Jager *et al.* 1993). The Forties Sandstone Member represents the primary reservoir unit in the majority of hydrocarbon accumulations situated on the Forties–Montrose High. The Nelson reservoir is subdivided into five fourth-order sequences Z1 to Z5, of which Z5 is the youngest, based on detailed biostratigraphy supplemented by lithostratigraphy and seismic mapping (Fig. 2). Zones 3 to 5 can be equated to the upper unit of Whyatt *et al.* (1992) and zones 1 to 2 the lower unit. The boundary between the upper and lower Forties units often corresponds to a slump sheet containing large amounts of reworked Lista-aged sediments and is a field-wide seismic horizon. A secondary intra-reservoir seismic horizon equates to the top of Z3. The gross reservoir interval (Z1 to Z5) varies from 17 m to 140 m (56 ft to 459 ft) in thickness across the field with an average of 78 m (257 ft). The field is filled to spill, with a maximum oil column of 85 m (278 ft), and connects via a regionally extensive aquifer to the Forties Field to the north and the Montrose and Arbroath fields to the south (Fig. 1). Reservoir quality is typically excellent, with overall net:gross averaging 70%, porosity 23% and zonal average permeabilities ranging from 150 mD to 300 mD.

Sand deposition within the field has been concentrated into three distinct axial fairways, the west, central and eastern channel complexes (Fig. 3), which run in a NW–SE direction across the structure. The Central Channel system was active mainly during Z3 times, after which sedimentation shifted to the Western and Eastern Channel axes during Z4 times. Finally, sedimentation shifted to the east of the field during Z5 times. These channel axes demonstrate an offset stacking pattern, indicating that basin floor topography was an important control on sedimentation.

The reservoir was extensively cored during appraisal and development drilling with approximately 2000 m (6500 ft) of core taken to date from 25 wells. The large amount of core material has allowed detailed sedimentological and petrophysical analysis of the field. The sediment gravity flow classification scheme of Mutti & Ricci-Lucchi (1975) has been used to carry out facies analysis on core data from the field. The main sediment fairways are comprised mainly of Facies A and B, indicating that fairway deposition was dominated by high-density turbidity currents. Towards the edges of the fairways, sediments are seen to comprise more heterolithic facies with lesser amounts of Facies B, and increased amounts of Facies C and D. With increasing distance from the channelized fairways thin-bedded Facies D predominate. An example of the cored

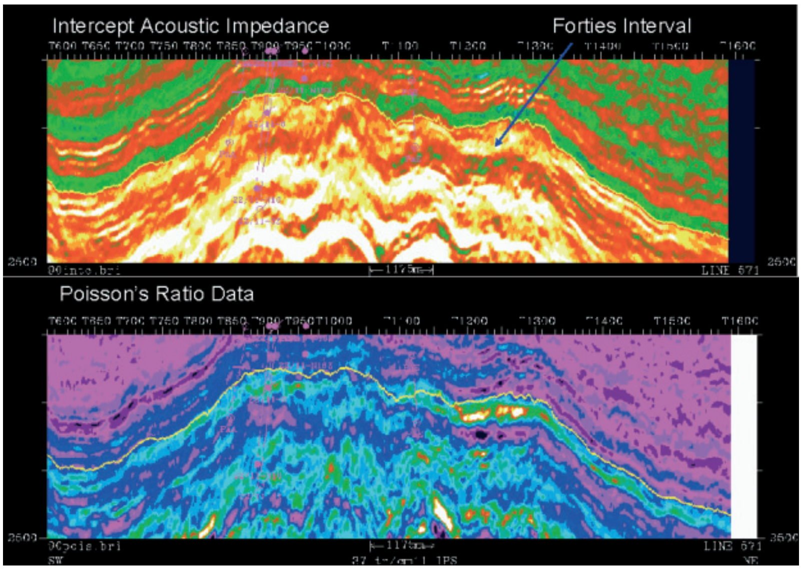

Fig. 8. Examples of the acoustic impedance and Poisson's ratio inversion results. The top of the Forties interval is shown as the yellow horizon. Reds and yellows in the acoustic impedance section are indicative of sandstones, greens are indicative of shales. Greens, yellows and reds in the Poisson's ratio section are indicative of low Poisson's ratio sandstones; these are oil bearing in the Forties interval.

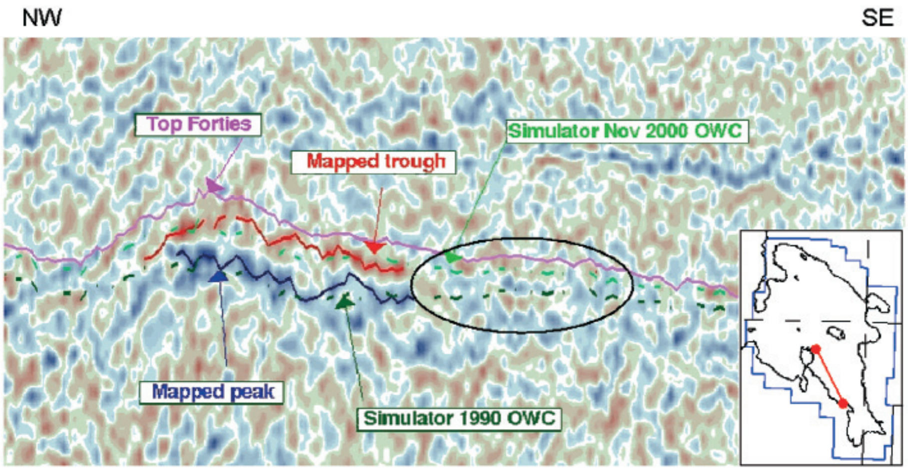

Fig. 9. A conventional far-offset difference display showing the typical trough (red)– peak (blue) 4D signature.

facies from channel margin producer N16Y is shown in Figure 4. Channel margin wells, such as N16Y, display the best production characteristics due to the combination of high permeability channel sands which maintain high oil rate interbedded with laterally extensive shales which present vertical barriers to water movement (Fig. 5).

GEOPHYSICS AND AVO

The main Nelson sediment fairways within the Forties Sandstone Member are readily imaged on seismic data due to their high impedance contrast with the surrounding basinal shales (Fig. 6). The oil filling the Nelson reservoir is a relatively light crude (38°API), and is highly compressible with a gas/oil ratio of 540 SCF BBL^{-1}. Water-filled Forties Sandstone reservoir has a Class I AVO response. This moves to a Class II response when oil filled, causing a relative dimming of the Top Forties amplitude on stack data (Fig. 7). Oil-filled sands have a reduced P-impedance (approximately 8% lower) with respect to water-filled sands and demonstrate a phase reversal at far offsets (>2500 m) *c.* 25° angle of incidence. Data acquisition at far offset is limited by the intersection of top reservoir reflector moveout with the Top Chalk reflector below, which has a significantly higher moveout velocity. The prestack seismic data are generally of good quality; however, near offset traces in particular are prone to noise in the form of residual multiples. In order to suppress residual noise for AVO interpretation sub-stacks are created from near and far offsets, greatly enhancing the signal to noise ratio and the AVO signal.

To date, three 3D seismic surveys have been shot over the Nelson Field. The original seismic data were acquired in 1990 during the appraisal stage of the field. In 1997, three years after original production start-up (approximately 200×10^6 BOE produced), a dedicated time-lapse monitoring survey was acquired and a further 4D survey was acquired in 2000 (300×10^6 BOE produced). An excellent review of the early work on the Nelson 4D data prior to the 2000 data acquisition is given in Boyd-Gorst *et al.* (2001). The timing of the 4D acquisition, in August and September of 2000, has been critical to the successful application of the technology to the subsequent infill drilling campaign, which started in mid-2001. The 4D data were acquired as close as possible to the start of infill drilling, while still allowing adequate time for processing and interpretation. The timing allowed the 4D project to have maximum impact throughout the drilling campaign, through risk mitigation and the identification of new targets.

The Nelson Reservoir Development Team has adopted an integrated approach to 4D seismic interpretation and reservoir characterization in order to optimize the analysis of the numerous seismic data volumes available. 4D seismic data

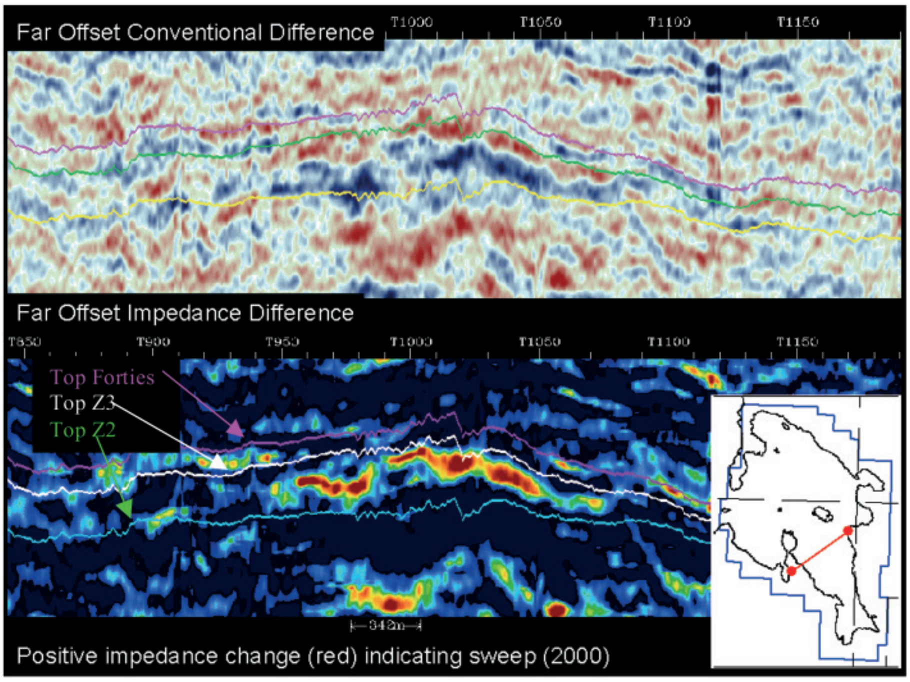

Fig. 10. Shows a comparison of the conventional far-offset difference data to the inverted far-offset difference data. In the lower section bright colours indicate a positive impedance change. The difference signal is restricted to the lower Z3 reservoir interval (see Fig. 2).

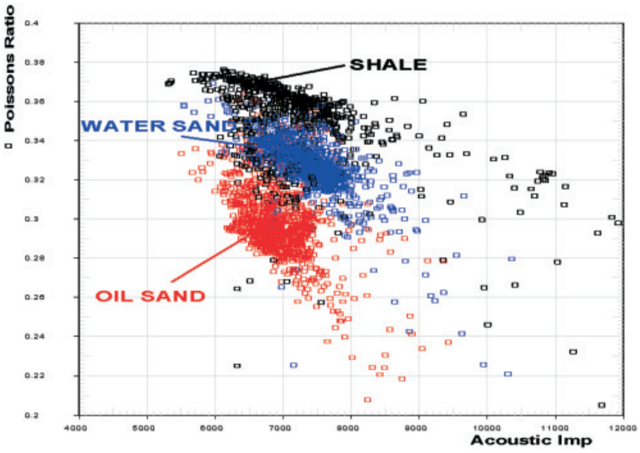

Fig. 11. Cross-plot of Poisson's ratio versus acoustic impedance for well log data from the Nelson reservoir interval. Oil- and water-filled sands, as well as shale fields, can be clearly defined.

cannot be interpreted in isolation from reservoir characterization (geology, petrophysics, geophysics and reservoir engineering data) since the sweep signal is strongly dependent on the local reservoir quality. An absence of 4D signal in an area could be due to lack of sweep in excellent reservoir, or just a lack of good reservoir (swept or unswept). It is obviously paramount to distinguish between the two possibilities when screening 4D infill opportunities. In order to help achieve these twin aims it was decided to undertake full elastic inversion of the conventional AVO seismic data.

ELASTIC INVERSION

Elastic inversion of the three vintages of the Nelson seismic data (1990, 1997, 2000) has been undertaken. The elastic inversion process uses the concept of angle (or elastic) impedance (Z_θ) (Resnick 1993; Connolly 1999) which allows the inversion of offset or angle stack seismic data using the convolutional model (equation 1). This method allows a more quantitative approach to seismic interpretation than conventional AVO analysis, which is prone to seismic noise (Swan 1993; Hendrickson 1999; Simm *et al.* 2000). Inverting sub-stacks for AVO analysis has three main advantages over conventional AVO analysis. The inversion process removes wavelet effects, suppresses random noise (in this case by application of a cost function) and improves bandwidth compared to the original seismic data (Cooke & Schneider 1983). Bandwidth can also be matched across the offset range due to the use of independent wavelets for each sub-stack. In addition there are also interpretational advantages and geological insight to be gained from the volume interpretation and visualization of layer-based impedance datasets. Full inversion also has several advantages compared with a SAIL inversion (Lindseth 1979) or 'coloured' inversion approach (Lancaster & Whitcombe 2000) which do not explicitly deconvolve the wavelet and therefore contain residual tuning phenomena and are less efficient at attenuating random noise.

$$Z_\theta = Z_p exp([\log(Z_p) - 2(\log(Z_s) + C]\sin^2\theta) \qquad (1)$$

From Hansen *et al.* (2001), where Z_p is acoustic or P-wave impedance, Z_s is shear impedance and C is a constant.

The first step in the inversion process is to calculate appropriate angle impedance logs for each offset stack angle by varying the effective angle, θ, in equation (1) and calculating the resulting offset reflection coefficients. In this case the near and far offset stacks correspond to approximately 12° and 25° at the reservoir level. Shear velocity data required for the angle impedance calculation are not available on all Nelson wells so a shear velocity predictor was used in the calculations (Boyd-Gorst *et al.* 2001). The reflection coefficient series can then be used to estimate wavelets, for example using a least squares or similar method (White 1980). These wavelets are then used as the input for inversion. A different wavelet was used for each sub-stack; however, the same wavelets applied to the 1990 sub-stacks were used for the 1997 and 2000 vintages due to the convergent processing. Simple inversion of the offset seismic data at this stage produces unbiased 'relative' impedance sections. These relative impedance sections are then scaled using low frequency impedance models derived from well data

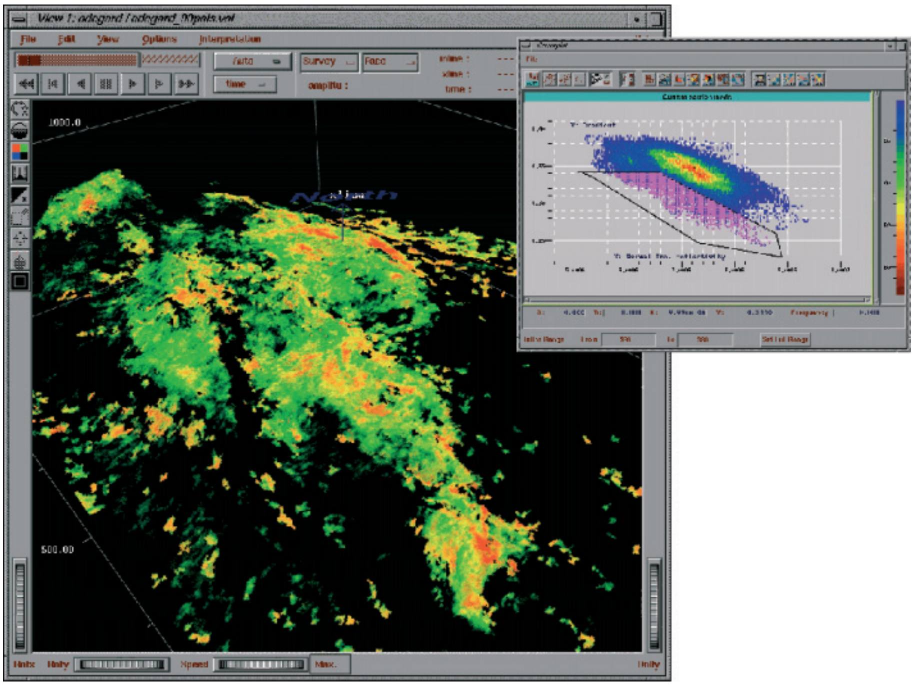

Fig. 12. Perspective view to north showing a volume detection of the 1990 Poisson's ratio volume. The detected voxels were selected in Z_p vs. σ space corresponding to the oil sand field based on well log data (Fig. 11).

interpolated throughout the seismic volume guided by interpreted horizons from the seismic (Rasmussen & Maver 1996; Rasmussen 1999). This allows the inversion data to be interpreted in terms of absolute impedance, which can be directly compared with well data. In this case, the low impedance model was built from well logs from nine near-vertical wells across the field. The predicted absolute impedance volumes were then tested against two 'blind' wells which were not used in model construction.

Acoustic impedance (Z_p), shear impedance (Z_s) and Poisson's ratio (σ) can be derived from offset stack inversion results by estimating the optimum linear relationship in the $\log Z_\theta, \sin^2\theta$ domain. Z_p is calculated at θ=0° and s values are calculated from the angle impedance at θ=90° (equation 1). The estimation of Poisson's ratio is additionally constrained by a low frequency impedance model calculated from the well log data. The constraint is used to dampen non-physical fluctuation appearing in the estimate of Poisson's ratio values due to seismic noise. Figure 8 shows some examples of the acoustic impedance and Poisson's ratio data.

The predicted acoustic impedance, shear impedance and Poisson's ratio volumes form the basis of our approach to fluid and lithology prediction in the Nelson Field.

Mapping OWC movements

Previous work on the Nelson Field showed that far offset AVO volumes from the various vintages of seismic data (1990, 1997 and 2000) are most responsive to fluid movement, and have greater amplitudes than zero offset data (Boyd-Gorst *et al.* 2001). Moreover, the far offset products show the fluid properties but are insensitive to pressure effects (Boyd-Gorst *et al.* 2001). For this reason, the 4D signature has been interpreted on the far offset difference data. Simple synthetic 4D far offset difference models have been used to constrain the form and resolution limits of the 4D signature with respect to reservoir quality, oil column thickness, and to relate the 4D signature to OWC movement. The offset models were constructed using variations on Connolly and Whitcombe's Elastic Impedance equations (Connolly 1999, Whitcombe *et al.* 2002). In the

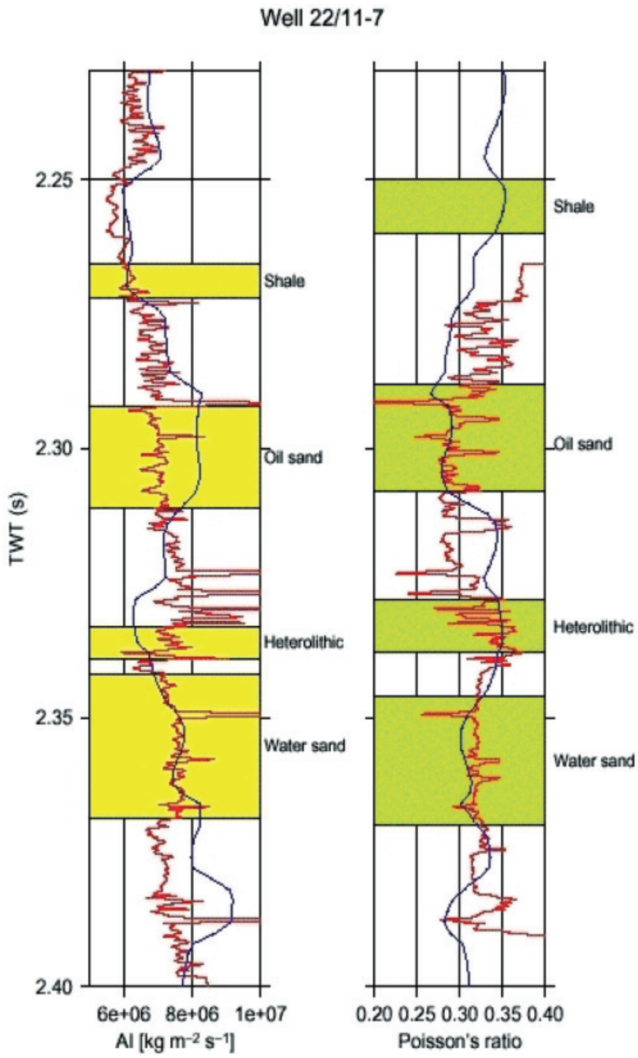

Fig. 13. Z_p and Poisson's ratio volumes are carefully calibrated to well log data to account for systematic shifts in absolute value and inversion bandwidth/resolution.

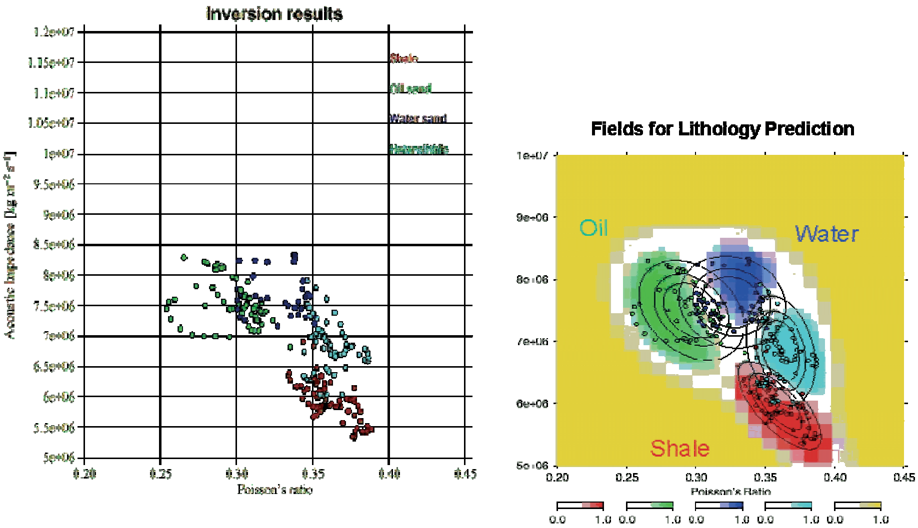

Fig. 14. Defining lithology and fluid fields from inversion data to carry out a probabilistic prediction of fluid and lithology volumes.

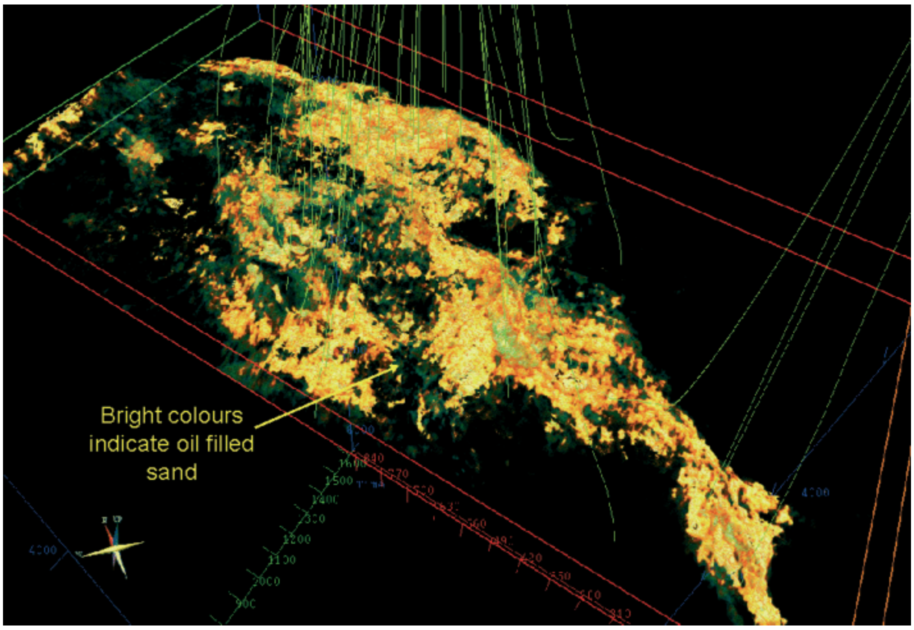

Fig. 15. A perspective view to the northeast of the oil sand volume prediction from the 1990 baseline acoustic impedance and Poisson's ratio data.

Nelson Field a trough/peak 4D signature is observed in the far offset conventional difference (1990–2000) (Fig. 9) (Redondo-Lopez *et al.* 2002; MacBeth *et al.* 2002). The trough corresponds to the moved OWC and the peak corresponds with the original OWC (Redondo-Lopez *et al.* 2002). The trough/peak signature has been mapped throughout the far offset difference volumes for use in the prediction of moved OWC in reservoir simulation history matching and delineation of sweep.

In the far offset elastic inversion difference data the moved OWC becomes a negative to positive impedance contrast due to oil being replaced by water within the reservoir (see below). In addition the 4D signal within the inversion difference data is confined within the area where sweep is actually taking place, aiding the visualization and interpretation of sweep within the reservoir (Fig. 10). Additionally comparison of moved OWC surfaces from the 4D seismic and the simulator can highlight areas of agreement and divergence (Fig. 9). The seismic isochron from Top Forties to the 4D moved OWC also shows an excellent linear relationship to remaining oil column measured from time-lapse production logs. This has allowed quantitative predictions of the remaining oil column to be made at infill locations (Redondo-Lopez *et al.* 2002). Results from the infill campaign to date have shown these predictions to be accurate to the order of 15 ft (4.5 m).

Through mapping of the moved OWC in the far offset inversion difference volumes, it has been possible to constrain the spatial extent of the 4D signature. The spatial distribution of the 4D signal correlates closely with areas of high net:gross (>0.65), corresponding to the Eastern, Central and Western Channel complexes (Redondo-Lopez *et al.* 2002). However, if no 4D signature is detected within the reservoir interval it may indicate that the reservoir is unswept or is of poor quality. Interpretation of the 4D signatures therefore has to be carried out in conjunction with fluid and lithology prediction studies, as discussed below, to be able to discern between those two possibilities.

OPTIMIZING FLUID AND LITHOLOGY IMAGING ON 4D SEISMIC DATA

With a multitude of seismic volumes available from three different seismic vintages, and associated differences, it is important to recognize which inversion products will contain dominant lithology or fluid information. This analysis is best

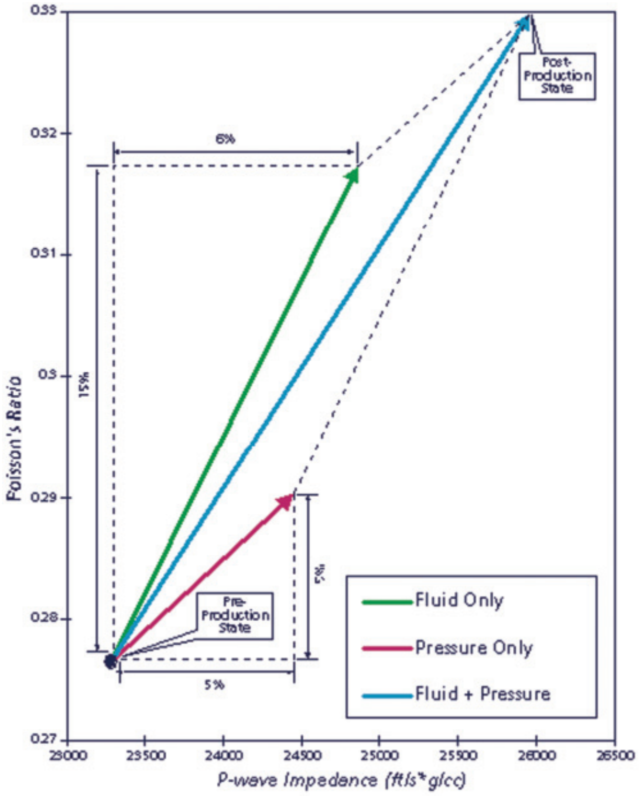

Fig. 16. Combined pressure and saturation response for a typical Nelson sandstone (J. Boyd-Gorst, pers.comm.).

carried out using well log data prior to seismic inversion in order to streamline the inversion process. Petrophysical analysis of borehole and invasion-corrected well log data from the reservoir interval of the Nelson Field shows that fluid and lithology effects cannot be isolated on any individual inversion dataset. However, distinctive fields for oil sand, water sand and shale can be defined in the combined acoustic impedance/ Poisson's ratio (Z_p vs. σ) parameter space (Fig. 11). This clear separation indicated that it may be possible to isolate fluid and lithology volumes from the inversion data in a similar manner using multiple inversion volumes (Fig. 12). Direct comparison of absolute values of Z_p and σ from the seismic volumes at well locations, with well data has shown that there are small but significant systematic differences between the two datasets. In order to correct for these minor systematic shifts, caused by the limited bandwidth of the inversion data, careful calibration was made between lithologies identified on well logs in Z_p vs. σ space and those from the seismic data (Fig. 13). The samples for the corresponding fluid and lithology fields were used as input to a probabilistic prediction of fluid and lithology from the seismic volumes. The statistical distribution of each fluid and lithology field was analysed to define mean value and co-variance, assuming a Gaussian distribution. Probability density functions are then calculated for each fluid and lithology field and contoured (Avseth *et al.* 1998; Mukerji *et al.* 1998) (Fig. 14). This allows the probability of a given inversion Z_p vs. σ pair of belonging to a given lithology class to be determined resulting in 'probability volumes' (Hansen *et al.* 2001). The lithology volumes were calculated for each seismic vintage (1990, 1997 and 2000). Figure 15 shows a 3D view of an oil sand probability volume predicted for the 1990 baseline survey.

In order to evaluate the effects of production in Z_p vs. σ space, fluid substitution and dry-frame pressure relationships were used to calculate changes in Z_p and σ due to changes in saturation and reservoir pressure (see Boyd-Gorst *et al.* 2001) on well log data. Figure 16 shows that changes in Z_p and σ are dominated by changes in oil saturation, and that reduction in reservoir pressure and decreasing oil saturation are additive (Boyd-Gorst *et al.* 2001). The seismic inversion results show a similar response due to production to that expected from the well log information. Figure 17 shows a vector plot of the change in Z_p vs. σ calculated from the 1990 and 2000 seismic inversion data, indicating that the inversion data from the different vintages is reflecting production changes and could be used as a direct indicator of reservoir sweep. Figure 18 shows a comparison of trace data from the oil and water probability volumes for each of the three surveys extracted along the path of a producing well with production log data. The probability traces were plotted against time-lapse water saturation curves derived initially from open-hole resistivity logs, and subsequently from cased-hole neutron logs. The oil probability from the 1990 survey compares well with the initial oil column logged before production start-up. Also, the oil probabilities from the 1997 and 2000 surveys show a good comparison with the reduced oil columns logged through casing in 1997 and

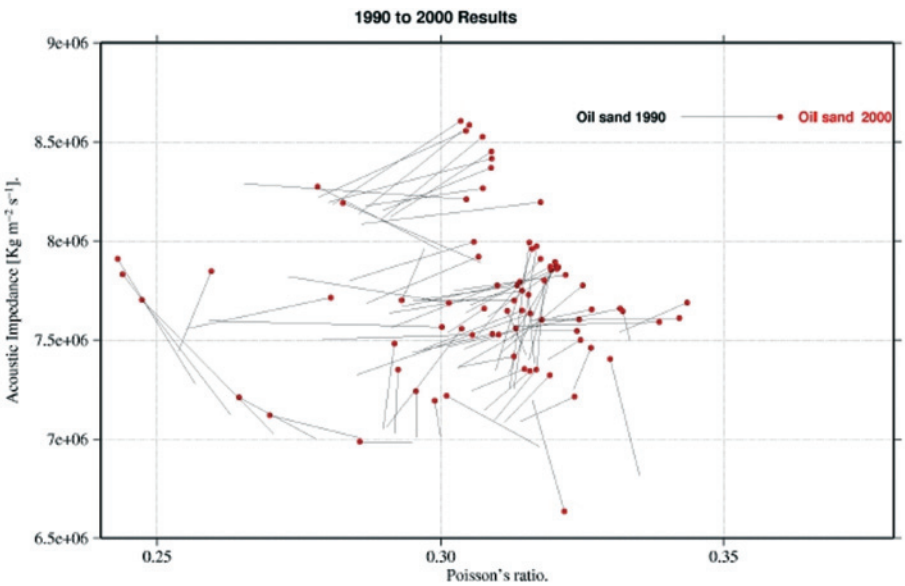

Fig. 17. A vector plot showing the change in Z_p vs. σ pairs predicted from seismic data between 1990 and 2000. The vectors compare favourably to predicted changes in Figure 16.

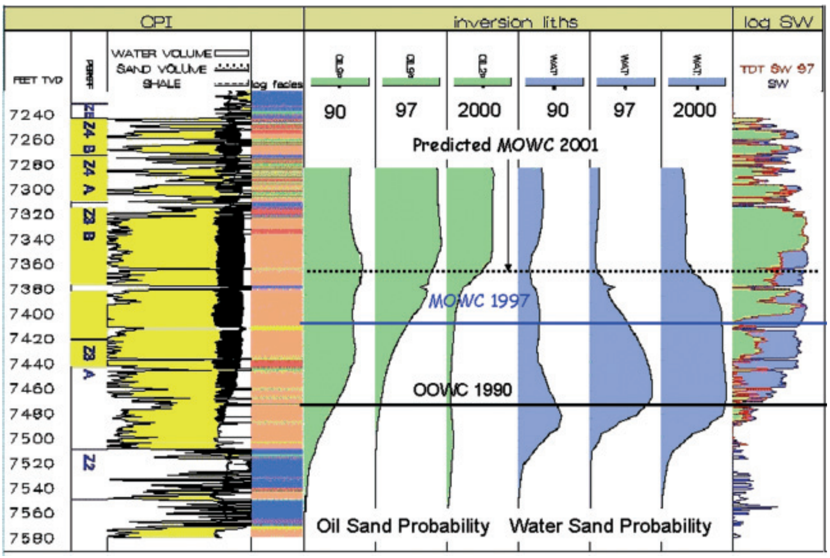

Fig. 18. Comparison of water saturation changes from a central channel production well to changes in oil and water probability at the same location.

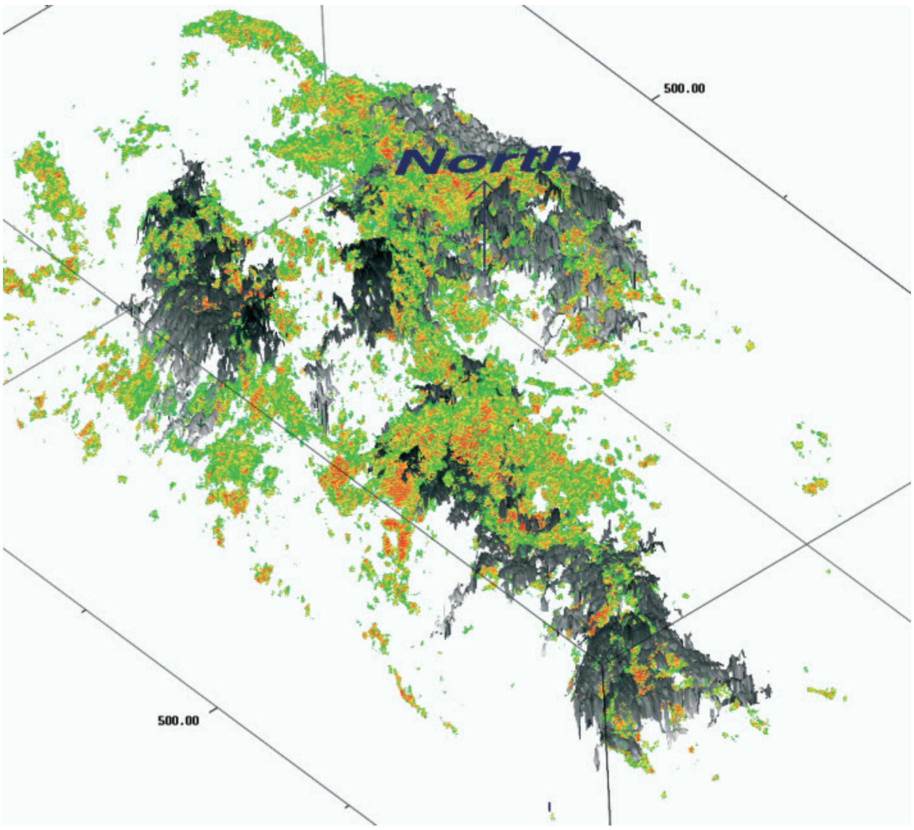

Fig. 19. Isometric perspective to view to the north of a volume detection of high oil sand probability (bright colours) masked by a detection of positive impedance change (2000–1990) in grey. Bright colours indicate potential unswept oil at the top of the reservoir at mid-2000.

2000. Furthermore, it can be seen that the reduction in oil probability has been replaced with an increase in water probability. Hence the movement in the OWC at this location almost perfectly matches the movement observed at the same time steps by cased-hole logs. This technique has the potential to be used as a seismic production log, particularly in areas of operational constraint such as subsea wells and tiebacks where acquisition costs for production information are prohibitive.

INTEGRATED VOLUME INTERPRETATION

The main objective of our approach to fluid and lithology imaging is to identify infill opportunities within the Nelson Field – areas of good quality reservoir which are unswept. In order to identify these areas, volume interpretation techniques are applied to multiple seismic volumes simultaneously. These techniques radically improve interpretation turn-around times, giving rapid results and allowing more efficient integration. Amplitude detection of high oil sand probability and high impedance change are extracted to capture areas of good reservoir which have been swept (Fig. 19). The remaining areas, which exhibit high oil probability and no impedance changes, are highlighted as possible infill targets. These possible targets are then cross-checked with the reservoir simulator by direct comparison of moved OWC surfaces from 4D seismic and reservoir simulator (Fig. 9). In areas where there is close

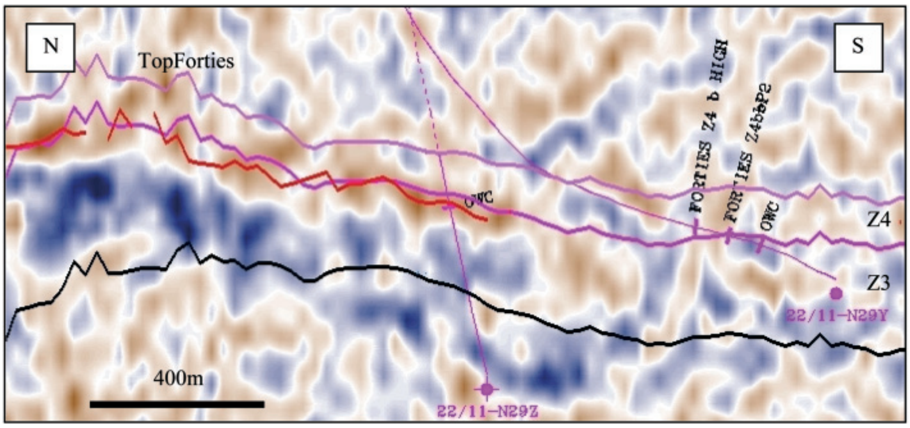

Fig. 20. Pre-drill predictions from 4D data and simulator for the N29z and y pilot and production wells indicated that the Z4 section would be unswept. The pilot hole, N29z, encountered the moved OWC within 10 ft of prognosis (red horizon). The N29y well encountered 1000 ft of excellent Z4 reservoir section and produced at initial rates of 11 500 BOPD.

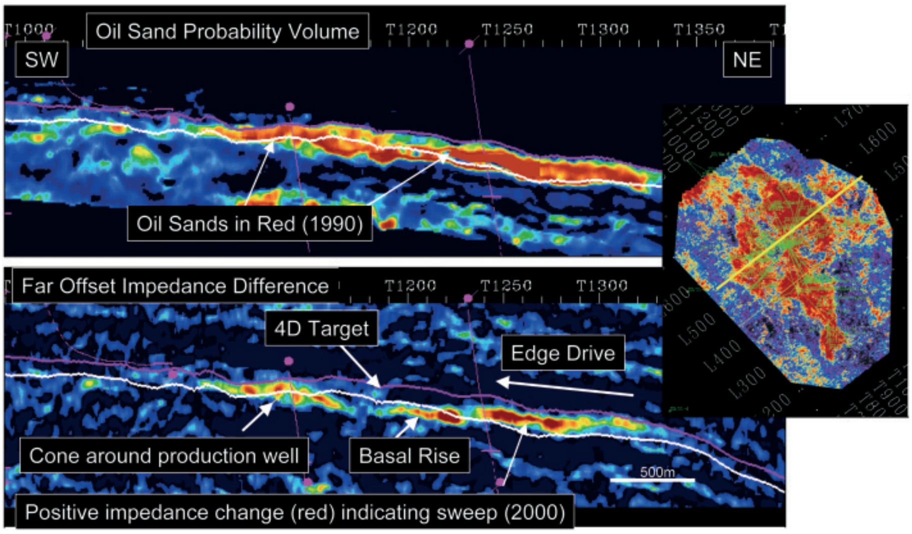

Fig. 21. Oil sand probability and far-offset impedance difference sections through the N30 target, between two nearby production wells. It can be seen from the sweep pattern on the far-offset impedance section that oil is not being swept effectively from the Z4 section between the two producers, in an area which the oil sand probability shows to be good reservoir.

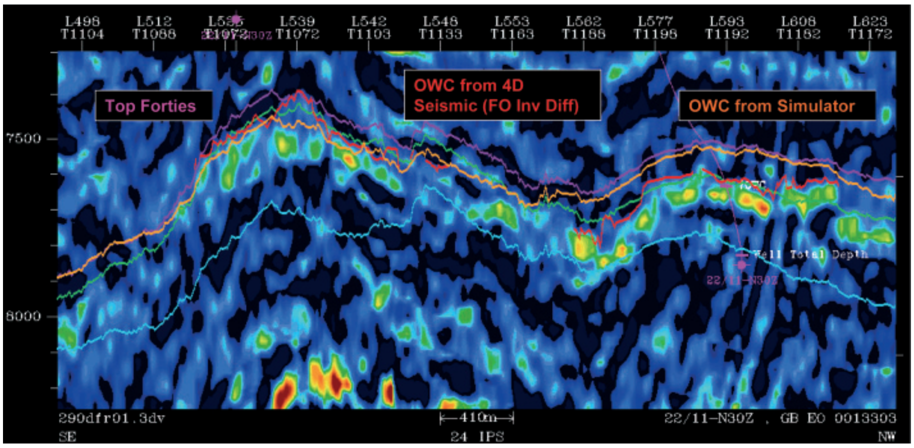

Fig. 22. Far-offset impedance difference section intersecting the N30y production well. Bright colours show a high positive impedance contrast (sweep). The pilot hole for the well encountered an 80 ft oil column before penetrating the moved OWC as prognosed by 4D data. Simulation had indicated that the area would be almost completely swept (orange horizon).

agreement between seismic and simulator-moved OWCs, the simulator is used to quantify incremental reserves and economics. This methodology has been validated by a recent infill well (Fig. 20) which encountered a high net:gross unswept channel sandstone section in the south centre of the field. In addition to targets verified in the reservoir simulator, the 4D method has also the potential to uncover targets which appear swept in the simulator. One such infill opportunity has been drilled recently (Figs 21 and 22). The 4D data showed this region to be a high net:gross unswept area with a predicted oil column of 25 m (80 ft) versus only 3 m (10 ft) predicted from the simulator. In these cases the incremental reserves and economics of the unswept targets are evaluated by volume detection.

Volumetric calculations can be carried out from amplitude detections of the seismic data, for example voxel detection of high amplitudes in the 4D far offset inversion data, have also been used to calculate produced hydrocarbons from the field (Fig. 19). This calculation was very close to the total field production (within 10%) at the time of 4D acquisition. Since the 4D signature is only detected within the main channel fairways, the calculation indicates that only these areas of the field are being exploited, thus suggesting significant remaining potential in interchannel and channel margin. Wells in channel margin areas in particular have proven to have excellent production characteristics (Fig. 5) and additional targets in these areas are currently being evaluated.

CONCLUSIONS

Elastic inversion of three vintages of 4D seismic data has been successfully implemented on the Nelson Field, UKCS, to produce volumes of acoustic impedance, shear impedance and Poisson's ratio. Elastic inversion has several advantages over conventional AVO and 4D analysis, including removing wavelet effects, suppressing random noise and improving geological understanding. The elastic inversion data, in conjunction with petrophysical analysis, have been used to produce optimized volumes for fluid and lithology imaging based on probabilistic prediction. The technique uses well-derived relationships in the Z_p vs. σ parameter space, which separate oil sand, water sand and shales. These optimized volumes also provide valuable insights into the sedimentary architecture. At the same time, important information regarding the sweep pattern of the field is gained through interpretation of 4D difference data. This facilitates making better decisions concerning development opportunities, such as infill locations, by identifying uswept areas of good reservoir quality. Infill results from six wells drilled through 2001–2002, have validated the use of 4D data on the Nelson Field, by adding incremental reserves and contributing to a 20% rise in field production at the time of publication. Four-dimensional technology, elastic inversion and fluid and lithology prediction has also had the additional benefit of encouraging closer multidisciplinary collaboration, showing that geophysics has an invaluable role in field development.

The authors would like to thank the Nelson Field partners Shell UK Ltd, ExxonMobil International Ltd, TotalFinaElf Exploration UK plc, Intrepid Energy North Sea Ltd, Svenska Petroleum Exploration and Summit North Sea Oil Ltd, and their respective representatives, for their support and publishing permission. Gail Riekie, John McGuckin, Steve Burford, Marie Luise Jensen and Liz Pointing from the Operated Fields Team at Enterprise Oil plc are also thanked for many fruitful discussions and critical input. Lorna Donald and Barry Glennie are thanked for the drafting of figures.

REFERENCES

Ahmadi, Z.M., Sawyers, M., Kenyon-Roberts, S., Stanworth, C.W., Kugler, K.A., Kristensen, J. & Fugelli, E.M.G. 2003. Paleocene. *In:* Evans, D., Armour, A., Bathurst, P. & Graham, C. (eds) *The Millennium Atlas: petroleum geology of the central and northern North Sea.* Geological Society, London, 235–260.

Avseth, P., Mukerji, T., Mavko, G. & Veggeland, T. 1998. Statistical discrimination of lithofacies from pre-stack seismic data constrained by well log rock physics: Application to a North Sea turbidite system. *Society of Exploration Geophysics Annual Meeting, New Orleans, Expanded Abstracts.*

Boyd-Gorst, J., Fail, P. & Pointing, L. 2001. 4D time lapse reservoir monitoring of the Nelson Field, Central North Sea: Successful use of an integrated rock physics model to predict and track reservoir production. *The Leading Edge,* **20**(12), 1336–1350.

Connolly, P. 1999. Elastic Impedance. *The Leading Edge,* **18**(4), 438–452.

Cooke, D.A. & Schneider, W.A. 1983. Generalised linear inversion of reflection seismic data. *Geophysics,* **48**, 665–676.

Den Hartog Jager, D., Giles, M.R. & Griffiths, G.R. 1993. Evolution of Paleogene submarine fans of the Northe Sea in space and time. *In:* Parker, J.R. (ed.) *Petroleum Geology of Northwest Europe: Proceedings of the 4th Conference.* Geological Society, London, 59–71.

Hansen, L., Davies, D., Garnham, J., McInally, A. & Boyd-Gorst, J. 2001. Time-Lapse Lithology Prediction in the Nelson Field. *First Break,* **19**(1), 40–45.

Harris, P.E. & Henry, B. 1998. Time lapse processing: A North Sea case study. *Society of Exploration Geophysics Annual Meeting, New Orleans, Expanded Abstracts.*

Hendrickson, J.S. 1999. Stacked. *Geophysical Prospecting,* **47**(5), 663–705.

Jack, I. 1998. *Time-lapse seismic in reservoir management.* Distinguished Instructor Short Course. Society of Exploration Geophysics, Tulsa, OK.

Knox, R.W.O'B. & Holloway, S. 1992. 1. Paleogene of the Central and Northern North Sea. *In:* Knox, R.W.O'B. & Cordey, W.G. (eds) *Lithostratigraphic nomenclature of the UK North Sea.* British Geological Survey, Nottingham.

Koster, K., Gabriels, P., Hartung, M., Verbeek, J., Deinum, G. & Staples, R. 2000. Time-lapse seismic surveys in the North Sea and their business impact. *The Leading Edge,* **19**(3), 286–293.

Lancaster, S. & Whitcombe, D. 2000. Fast-track 'coloured' inversion. *Society of Exploration Geophysics Annual Meeting, Calgary, Expanded Abstracts.*

Lindseth, R.O. 1979. Synthetic sonic logs – a process stratigraphic interpretation. *Geophysics,* **44**(1), 3–26.

MacBeth, C., Reid, F., McInally, A., Garnham, J. & Redondo-Lopez, T. 2002. 4D seismic signatures of OWC movement on the Nelson field – modeling and interpretation. *Society of Exploration Geophysics Annual Meeting, Salt Lake City, Expanded Abstracts.*

Mukerji, T., Jorstad, A., Mavko, G. & Granli, J.R. 1998. Applying statistical rock physics and seismic inversions to map lithofacies and pore fluid probabilities in a North Sea reservoir. *Society of Exploration Geophysics Annual Meeting, New Orleans, Expanded Abstracts.*

Mutti, E. & Ricci-Luchi, F. 1975. Turbidite facies and facies associations. *In:* Mutti, E. (ed.) *Examples of turbidite facies and facies associations from selected formations of the Northern Appenines.* IX International Congress on Sedimentology, Nice, A-11, 21–36.

Parr, R.S., Marsh, M. & Griffin, T. 2000. Interpretation and integration of 4-D results into reservoir management, Schiehallion Field, UKCS. *Society of Exploration Geophysics Annual Meeting, Calgary, Expanded Abstracts.*

Rasmussen, K.B. 1999. Use of dip in seismic inversion. *EAGE Annual Conference Abstracts.*

Rasmussen, K. B. & Maver, K. G. 1996. Direct inversion of porosity of post stack seismic data. Paper SPE 35509. Society of Petroleum Engineers.

Redondo-López, T., McInally, A., Brooks, D. & Kunka, J. 2002. Quantitative integration of 4D Seismic for field development. *AAPG Meeting, Houston, Expanded Abstracts.*

Resnick, J.R. 1993. Seismic data processing for AVO and AVA analysis. *In:* Castagna, J.P. & Bavkus, M.M. (eds) *Offset-Dependent Reflectivity – Theory and Practice of AVO Analysis.* Investigations in Geophysics, **8**. Society of Exploration Geophysicists, 175.

Simm, R., White, R. & Uden, R. 2000. The anatomy of AVO crossplots. *The Leading Edge,* **19**(2), 150–155.

Swan, H.W. 1993. Properties for direct AVO hydrocarbon indicators. *In:* Castagna, J.P. & Backus, M.M. (eds) *Offset Dependent Reflectivity – Theory and Practice of AVO anomalies.* Investigations in Geophysics, **8**. Society of Exploration Geophysics, 78–92.

Whitcombe, D.N., Connolly, P.A., Reagan, R.L. & Redshaw, T.C. 2002. Extended elastic impedance for fluid and lithology prediction. *Geophysics,* **67**, 63–67.

White, R.E. 1980. Partial coherence matching of synthetic seismograms with seismic traces. *Geophysical Prospecting,* **28**, 333–358.

Whyatt, M., Bowen, J.M. & Rhodes, D.N. 1992. The Nelson Field: a successful application of a development geoseismic model in North Sea exploration. *In:* Hardman, R.F.P. (ed.) *Exploration Britain: Geological insights for the next decade.* Geological Society, London, Special Publications, **67**, 283–305.

Received 15 April 2002; revised typescript accepted 18 November 2002.